ISSN 1063-7834, Physics of the Solid State, 2017, Vol. 59, No. 3, pp. 620–628. © Pleiades Publishing, Ltd., 2017.
Original Russian Text © V.I. Berezkin, V.V. Popov, M.V. Tomkovich, 2017, published in Fizika Tverdogo Tela, 2017, Vol. 59, No. 3, pp. 601–609.

FULLERENES

Carbon Composite Based on Fullerenes and Exfoliated Graphite

V. I. Berezkin[a]*, V. V. Popov[b], and M. V. Tomkovich[b]

[a] *Research Center for Ecological Safety, Russian Academy of Sciences, St. Petersburg, 197110 Russia*
[b] *Ioffe Institute, Russian Academy of Sciences, St. Petersburg, 194021 Russia*
**e-mail: v.berezkin@inbox.ru*

Received July 27, 2016

Abstract—A carbon composite material based on fullerenes and exfoliated graphite with different ratios (from 16 : 1 to 1 : 16 by weight) is synthesized and investigated. Samples are obtained by the introduction of C_{60} in a conductive matrix by means of heat treatment of initial disperse mixtures in a vacuum diffusion–adsorption process followed by cold pressing and annealing. It is shown that covalent bonds are formed between the fullerenes and the environment. The conductivity of the samples is quite high and ranges from a few to hundreds $(\Omega\ \text{cm})^{-1}$. The concentration of charge carriers (mainly holes) is $\sim 10^{19}$ to $10^{20}\ \text{cm}^{-3}$. It is concluded that the material obtained using these ratios of the components can be attributed to metal systems with structural disorder.

DOI: 10.1134/S1063783417030076

1. INTRODUCTION

It is known that composite materials generally consist of an enclosing matrix and a filler or alternating layers of different components or phases [1]. Constituent parts can be in mechanical contact or chemically bind. Composites have a number of unique properties, so they have been long and successfully used in various fields.

Carbon composites have gained special significance today because of the ability to create a variety of electronic devices on their basis. By alternating sp^2 and sp^3 domains of micro- and nanometer size, layered compositions of the type of metal–insulator–metal or metal–insulator–semiconductor can be obtained [2, 3]. Such structures are considered promising for applications, for example, in photodetectors and light-emitting devices, for use as cold cathodes, or for creating superconductors.

Superconductivity was found in a variety of carbon materials [1]. In particular, it is observed upon introducing atoms of some metals (alkali, alkaline earth, or rare earth) into the molecular fullerene structures (films, crystals, or powders polycrystalline) [4]. However, metal-intercalated fullerene superconductors are extremely unstable. In air, they rapidly (within fractions of a second [5]) lose their superconductivity, due to the oxidation of metal impurities.

One way to stabilize the superconducting state can be the creation of such composites in that doped fullerenes are placed in a conducting matrix and chemically bonded to it. A natural matrix (binder) for such a composite is another carbon structure. Since solid carbon exists in a wide variety of modifications, it is possible to select the one that will ensure the creation of composites with chemical bonds between components. With sufficient concentration of a superconducting phase in the material, it mainly determines the nature of its electrical conductivity.

The principal possibility of implementing this idea was first demonstrated in [6]. In [7], it was shown that effects typical of the superconducting state are observed in such a material. In general, a new class of carbon composites was presented in [6, 7], in which fullerenes and doping additives (donor and acceptor) were placed in a carbon matrix. Upon doping with sodium, a state was obtained, stable in air, interpreted as superconducting at temperatures $T \le 15$ K. These composites were synthesized using the "diamond" technology, that is, by exposing initial mechanical mixtures to high pressure and temperature. The mixtures contained fullerenes, hydrocarbon binders (naphthalene $C_{10}H_8$ and others), and compounds with doping elements. It is well known that the diamond technology is characterized by essential nonuniformity of a number of parameters in the synthesis zone (including pressure, temperature, and substance distribution), which leads to poor reproducibility.

In the present paper, we present nondoped materials similar to those synthesized in [6, 7], but obtained under conditions that allow greater homogeneity of parameters in the working area; some of their optical and electrical properties are studied.

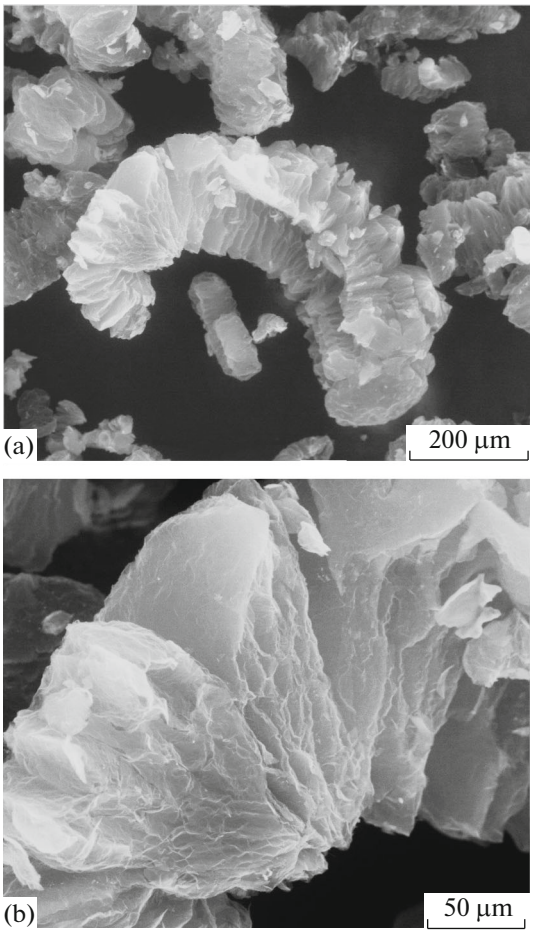

Fig. 1. Image of EG obtained by scanning electron microscopy: (a) a general view of a wormlike particle, typical of EG; (b) its enlarged detail.

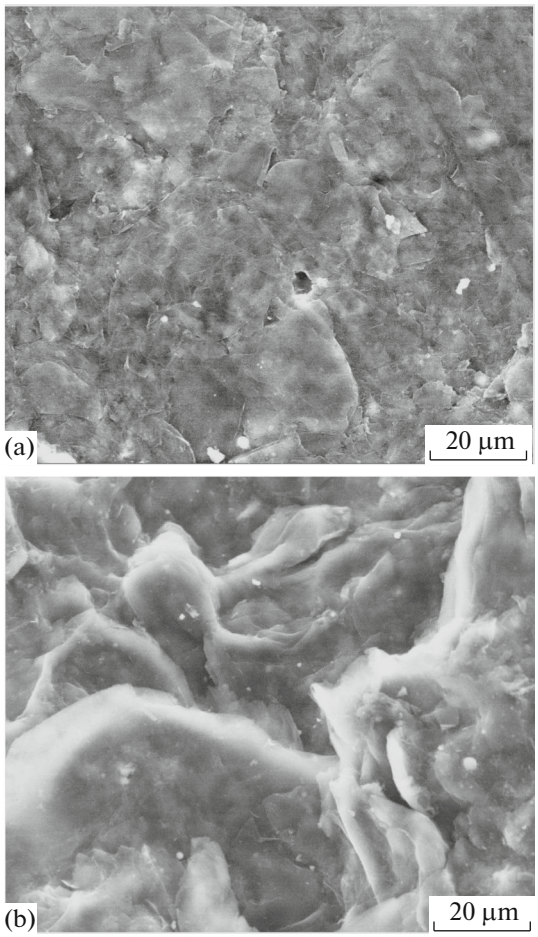

Fig. 2. Images of a EG sample compressed at 0.7 GPa: (a) surface, and (b) cleavage.

2. EXPERIMENTAL SAMPLES AND MEASUREMENTS

We used exfoliated graphite (EG) as a binder. It is prepared by rapid heating finely-ground graphite, usually natural (its density is 2.08–2.23 g/cm^3 [1]), intercalated with mineral acids (sulfuric or nitric). The graphite particles swell, and the distance between atomic layers increases hundreds of times. The result is a dispersed substance with very low bulk density (1.5–5.0 kg/m^3 [8]), comparable to the density of dry air (1.29 kg/m^3 at 0°C and 760 Torr [9]). An image of EG used in this work is presented in Fig. 1. It can be seen that it consists of individual particles with a distinct layered structure.

EG is suitable for cold forming (rolling, pressing) without binders. The result is flexible sheet materials including carbon foils and other products. They are of dark gray color with a matte sheen. Their density is in the range 0.5–1.6 g/cm^3; the most characteristic value is ~1.0 g/cm^3. In the densest samples, it can reach 2.16 g/cm^3. The densest compressed EG samples correspond in color and density to natural crystalline graphite of high quality. In other words, the chemical reaction of direct association ("polymerization") of EG particles into a low-porosity carbon monolith efficiently proceeds in a solid phase at room temperature ($T = T_{room}$). It may be noted that unlike EG, materials such as, for example, carbon black or activated carbons are not pressed without binders. Figure 2 shows the result of pressing EG at a pressure of 0.7 GPa. It is seen that a continuous solid structure is formed. Large surface pores are clearly visible in Fig. 2a (center and left).

Our research has shown that EG is a high-efficient carbon adsorbent, which is not inferior to active carbons. It may well accommodate fullerenes and other substances complying, under certain conditions, the role of a highly conducting medium-matrix and ensuring efficient electrical interactions of all components.

Regarding fullerenes, it is well known that their polycrystalline powders polymerize readily into rather strong monolithic samples under relatively low external pressures (up to 2 GPa) and also at $T = T_{room}$. For

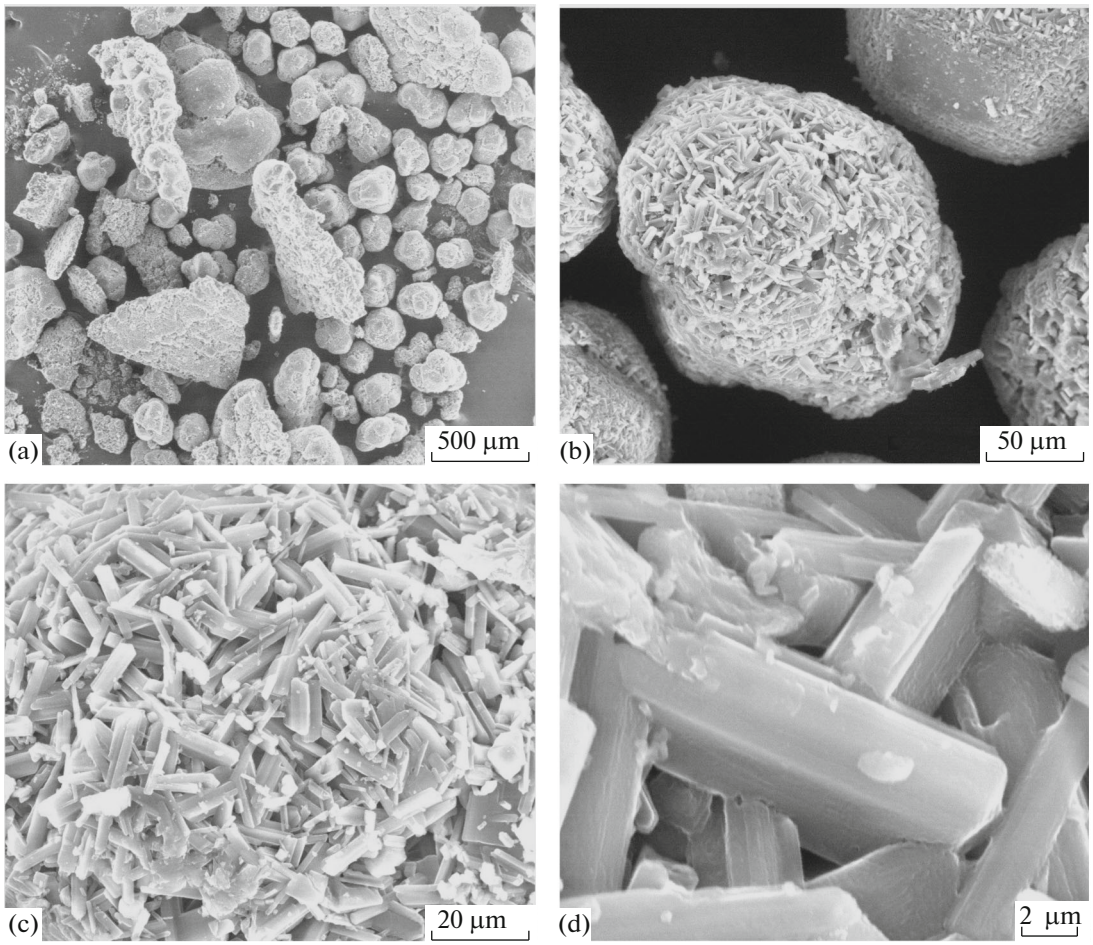

Fig. 3. Images of (a) polycrystalline powder of fullerene C_{60} and (b–d) its separate particle from the upper part of the photo at different magnifications.

example, the polymer phase is formed even at a pressure of 0.3 GPa [10]. For illustration, an initial polycrystalline powder of fullerene C_{60} is shown in Fig. 3. It is clearly seen that its particles consist of individual microcrystals. After exposure to external pressure of 0.7 GPa, such a microcrystalline structure is not observed (Fig. 4).

At elevated temperatures (from approximately 400°C and higher), initial fullerenes sublimate, and at 700–900°C (according to different authors [10]), their molecules begin to break regardless of the external pressure.

Considering all the above-noted, the following procedure was selected for synthesis. Mechanical mixtures of EG and polycrystalline C_{60} powders at their various ratios were placed in glass ampoules, which were evacuated with a backing pump and sealed off. This was followed by heating to 550–650°C for 0.5–1 h and holding for 5 h, so that fullerene C_{60} was evaporated, and the components were mixed in a rather long diffusion–adsorption process. After that, the oven was turned off, and the resultant dispersion products were cooled down in it. Then they were removed to air and pressed at a pressure of 0.7 GPa and $T = T_{room}$ into plates 13 mm in diameter and approximately 1 mm in thickness. Annealing of the plates (550–650°C, 5 h) was carried out in vacuum. Samples of the desired shape were cut out from the plates.

As a result, annealed and nonannealed samples were obtained at nine different initial ratios of C_{60} : EG, namely, 1 : 16, 1 : 8, 1 : 4, ..., and 16 : 1 (by weight). The typical image of the material is shown by the example of one of the synthesized samples in Fig. 5. It is seen that the sample is quite dense and homogeneous.

All the samples were of dark gray color with a matte sheen. A number of electrical, galvanomagnetic, optical, and other properties of these samples were studied. The dependences of resistivity $\rho(T)$ in the range of $T = 4.2$ K to $T = T_{room}$ and the Hall constant $R_H(H)$ at magnetic field $H = 0$–25 kOe and at $T = 77$ K were obtained. For this purpose, we used conventional four-probe procedures. The spectra of optical trans-

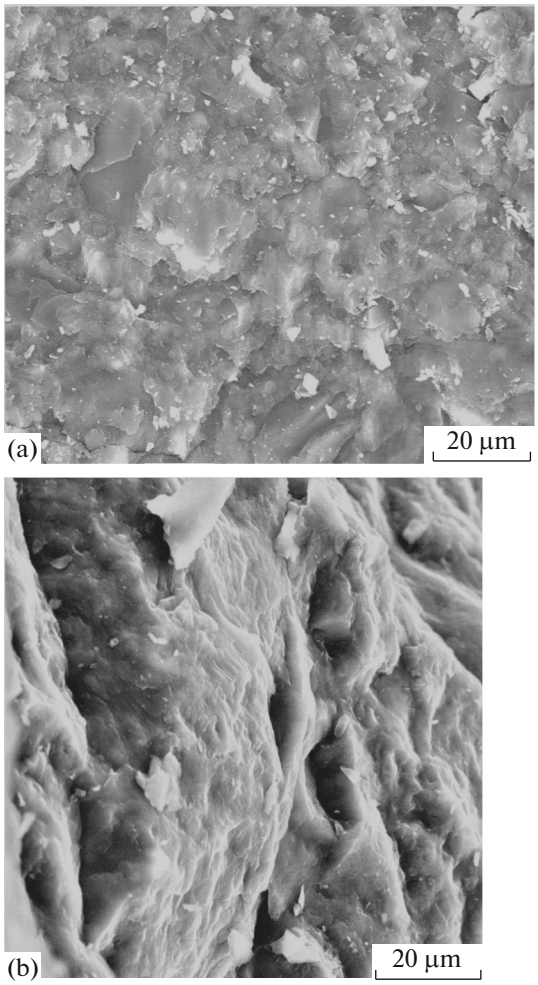

Fig. 4. Sample of polycrystalline powder of fullerene C_{60} after exposure to external pressure of 0.7 GPa: (a) surface, and (b) cleavage.

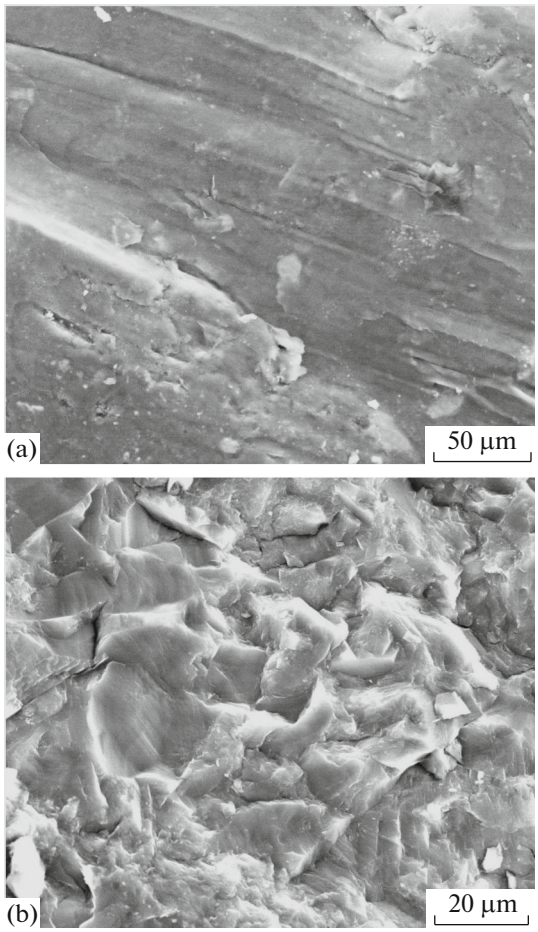

Fig. 5. Images of the synthesized C_{60} + EG composite material by the example of a sample with the initial weight ratio of components of 1 : 1: (a) surface, and (b) cleavage.

mission at $T = T_{room}$ in the range of frequency of the vibrational modes of a C_{60} molecule, namely, in the infrared (IR) range of 400–1500 cm^{-1}, were measured. A procedure conventional for such measurements was used: samples were crushed and pressed into KBr tablets.

For comparison, some parameters of samples prepared from pure EG and C_{60} were measured (samples of C_{60} were not annealed in order to avoid depolymerization).

3. RESULTS AND DISCUSSION

3.1. IR-transmission spectra. First, it should be found out whether the produced materials are simple mechanical mixtures of C_{60} + EG or there is a covalent bond, even partially, between the matrix and filler (that is, between the graphite particles and C_{60} molecules). A direct evidence of any of the results could be the data on the vibrational states of C_{60} molecules in the bulk samples. Such data are usually obtained by Raman scattering, IR spectroscopy, and neutron inelastic scattering. The fact is that when fullerenes form a covalent bond during polymerization or formation of compounds with other substances, the symmetry of C_{60} molecules (icosahedral group I_h) abruptly changes (decreases), so that substantial changes are observed in the spectra even at room temperature. In contrast, in molecular fullerene condensates, molecules rotate almost freely at $T = T_{room}$; therefore, the spectra do not differ from the corresponding spectra of a single molecule.

Vibrational modes of C_{60} were theoretically and experimentally investigated even in the initial stages of the study of fullerenes [11–15]. We omit their details characterization; recall only the main points that are important for the present study. In I_h symmetry, the degeneracy of 1, 3, 3, 4, and 5 is permitted. In the spectra, these modes are designated as A, T_1, T_2, H, and G, respectively. Indices g and u represent the tran-

sitions between the levels with conservation and change in the parity of the wave function. In a free C_{60} molecule, the number of internal degrees of freedom is 174. However, due to the high point symmetry of the molecule, only 46 vibrational modes are fundamental in accordance with the irreducible representations, namely,

$$\Gamma_{\text{mol}} = 2A_g(\text{R}) + 3T_{1g} + 4T_{2g} + 6G_g + 8H_g(\text{R}) + A_u + 4T_{1u}(\text{IR}) + 5T_{2u} + 6G_u + 7H_u. \quad (1)$$

Only ten modes of these are active ($2A_g + 8H_g$) in the Raman spectra (R) and only four T_{1u} mode are active in the IR absorption/transmittance spectra (IR). All of them are well noticeable in the spectra and can be easily recognized. In particular, optically active modes T_{1u} (1), T_{1u} (2), T_{1u} (3), and T_{1u} (4) are characterized in the IR spectra by frequencies 526, 576, 1183, and 1429 cm^{-1}, respectively. The remaining 32 modes are silent as forbidden by the selection rules. They do not appear or poorly appear in both Raman and IR spectra.

In the study of fullerene derivatives by vibrational spectroscopy, the data on IR spectra are often more preferable by a number of reasons. For example, this is due to the presence of extensive reference data on the IR spectra, which is useful for analyzing the structure of heteroromolecules attached to C_{60}, especially organic. With the help of IR spectra, fullerenes can be identified qualitatively: the long-wavelength absorption band at 526 cm^{-1} is the most suitable for the detection of C_{60}, as it is usually the most intense.

It is well known that by exposing fullerenes and their compounds to elevated pressures (including in combination with elevated temperatures), the intensity of this band relative to shorter-wavelength bands corresponding to other active modes may vary, and depending on the conditions, in both directions; that is, it may either decrease [16] or increase [17]. Silent modes can become active; there may be a splitting of IR lines due to removal of degeneracy; new bands may appear, including those of the type of overtones and complex oscillation (binary combinations of fundamental modes). The silent modes can be observed simultaneously in IR and Raman spectra (which is impossible for active modes) and in neutron spectra. According to [14], when C_{60} is exposed to even low pressures, up to 8 kbar (0.8 GPa), the shift in frequency of both active and silent modes may occur, which can be up to 20 cm^{-1}. In our samples, virtually all of these effects take place.

Typical IR transmission spectra measured at $T = T_{\text{room}}$ are given in Fig. 6. In all the dependences, features corresponding to IR-active vibrational modes are clearly visible. For initial (free) C_{60} (curve *1*), the intensity of the bands at 526, 576, 1183, and 1429 cm^{-1} are related as 1 : 0.60 : 0.27 : 0.24. After exposure to a pressure of 0.7 GPa (curve *2*), the ratio becomes

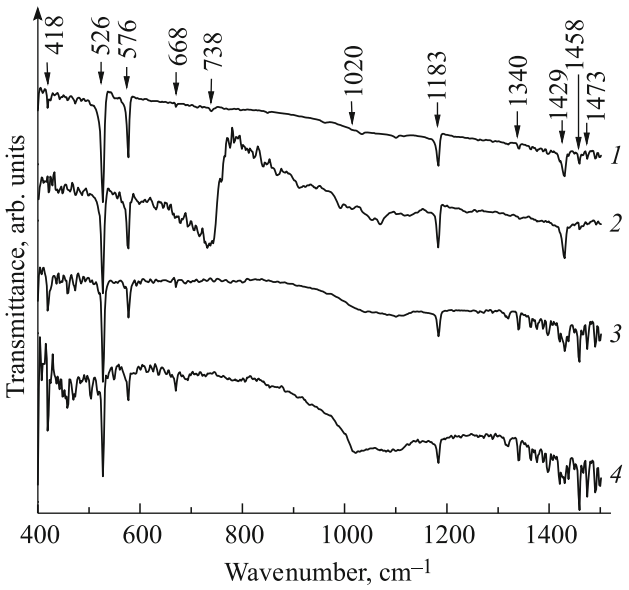

Fig. 6. Typical IR transmittance spectra (in arbitrary units) of the samples at $T = T_{\text{room}}$ in the frequency range of the vibrational modes of a C_{60} molecule. The arrows indicate the frequencies at which the features are located, mentioned in the text: (*1*) initial (free) C_{60}; (*2*) the same sample after exposure to external pressure of 0.7 GPa; (*3*) the sample synthesized at the initial composition of C_{60} : EG = 16 : 1; and (*4*) the sample obtained from the composition of C_{60} : EG = 1 : 4.

1 : 0.57 : 0.43 : 0.31. For the sample prepared from a mixture of C_{60} : EG = 16 : 1, we have the ratio of 1 : 0.37 : 0.24 : 0.26 (curve *3*), and for the composition of C_{60} : EG = 1 : 4 (curve *4*), it is 1 : 0.28 : 0.22 : 0.22. In other words, the relative change in the intensities of the permitted absorption bands of C_{60} clearly visible. Note that the annealing of the samples also lead to quite appreciable similar changes (up to 15% in either direction).

As for weak features, then, for example, a band at 418 cm^{-1} in curve *1* becomes highly developed in spectra *3* and *4*. It can be compared to mode $H_g(2)$, which is expressed in the rhombohedral polymer phase of C_{60} at 415 cm^{-1} [17]. Probably, mode H_g (2), silent in free C_{60}, becomes active in the samples of C_{60} + EG.

The weak feature in curves *1*–*3* at 668 cm^{-1}, corresponding to mode H_u (3), is clearly visible in curve *4*. On the right of it (692 cm^{-1}, curve *4*), a feature becomes noticeable that can be associated with a combination of two modes $H_u(1) + T_{2u}(1)$ with frequencies 342 and 353 cm^{-1}, respectively. Note that in [14], mode at 668 cm^{-1} in the initial C_{60} crystal at $T = 300$ K was also rather weak. In the same sample at $T = 77$ K (when the rotation of molecules is frozen), it is much more noticeable. After exposing the crystal to a high pressure of 25 kbar (2.5 GPa), it became highly visible

even at $T = 300$ K. In other words, both the cooling of C_{60} in [14] to a temperature below the glass phase transition ($T \approx 90$ K), at which the rotation of molecules is frozen, and the application of external pressure in [14] and in the present work have the same effect of this mode: both factors decrease the symmetry of the molecule. In the former case, it may occur due to the growing effect of the crystal field, defects and impurities, surface and isotope effects, etc. In the latter case, this is possible if after releasing the pressure, covalent bonds remain between C_{60} molecules in the crystal (at least, between some of them).

A barely visible feature at 738 cm^{-1} in curve *1* (Fig. 6), corresponding to mode G_u (2), is transformed in curve *2* into a strong broad absorption band with a central part split into four bands at 724, 730, 736, and 742 cm^{-1}. There are many small, but well-defined bands in curve *2* which can also be associated with a number of silent modes, including combined modes. For example, a combination of modes $H_g(1) + G_u(3)$ with the frequencies of 267 and 753 cm^{-1} correspond to the feature at 1020 cm^{-1}. It is barely noticeable in curves *1* and *2*, absent in curve *3*, and clearly visible in curve *4* at this frequency as a wide structureless band.

A weak band in curves *1* and *2* at 1340 cm^{-1} is very well visible in curves *3* and *4*. It corresponds to a combination of $T_{2g}(2) + H_u(2)$ with frequencies 764 and 579 cm^{-1}, respectively. A band of $T_{1u}(4)$ at 1429 cm^{-1}, resolved in the IR spectra, is clearly split into three bands in curves *3* and *4*; the lateral frequencies are 1419 and 1436 cm^{-1}.

Small features in curves *1* and *2* at 1458 and 1473 cm^{-1} are well developed in curves *3* and *4*. Both of these bands can be associated with the polymerization-sensitive mode $A_g(2)$, which, as seen from Eq. (1) is Raman-active in free C_{60} and silent in the IR spectra. In free C_{60}, this mode appears at frequencies close to 1470 cm^{-1}; it is characterized by different frequencies in various polymer phases. For example, in the orthorhombic phase, its frequency is 1457 cm^{-1} [17].

Thus, the phonon spectra of C_{60} in the samples vary considerably, which, in our opinion, can be considered a direct evidence of the presence of covalent bonds of fullerenes with the environment in these samples.

3.2. Porosity of the samples. The density of the obtained samples of C_{60} + EG is in the range from 1.27 g/cm^3 (C_{60} : EG = 16 : 1) to 1.74 g/cm^3 (C_{60} : EG = 1 : 16). The density of the samples from pure C_{60} is 1.50 g/cm^3, and the density of the samples from pure EG is 1.80 g/cm^3. Since the density of a C_{60} crystal is 1.69 g/cm^3 [18], and the theoretical density of graphite is 2.265 g/cm^3 [19], we can conclude that all of our samples are quite porous as indeed any other pressed materials, in contrast, for example, from fused ones. It is therefore important to know to what extent they are porous and how it may affect the electronic and other properties.

The relative porosity P of a material can be evaluated as follows. Its magnitude is

$$P = \frac{V_P}{V} = 1 - \frac{V_0}{V}, \quad (2)$$

where V_P is the pore volume, V_0 is the volume of the material, and $V = V_P + V_0$ is the total volume of the porous body. In multicomponent solids, volume V_0 is the sum of the volumes of initial components. In the case of two components with densities r_{01} and r_{02} and the mass content of m_1 and m_2 (here, these are the density of C_{60} and graphite single crystals), we can obtain from Eq. (2)

$$P = 1 - \frac{r}{r_{01}r_{02}}\left(r_{01}\frac{m_2}{M} + r_{02}\frac{m_1}{M}\right), \quad (3)$$

where $M = m_1 + m_2$ is the total mass of the sample, and $r = M/V$ is its measured density. Similar formulas can be easily obtained for a larger number of components. If there is one component, it follows from Eq. (3) that

$$P = 1 - \frac{r}{r_0}. \quad (4)$$

Estimates by Eqs. (3) and (4) show that in our samples of pure C_{60}, $P = 11\%$; in the samples with EG, $P = 14$–29% (average $P = 22$–23%); and in samples of pure EG, $P = 20\%$. For porous materials, these values are not high. In contrast, for such highly porous solids as activated carbons, the situation is reversed: the porosity is 70–80%; in other words, the material takes up only 20–30% of the total volume of the sample.

Measurements demonstrated that the resistivity of the samples (except for pure C_{60}) is low and in the range form units of (mΩ cm) to tenths of (Ω cm). This is orders of magnitude lower than that in the samples described in our previous studies [6, 7]. There, the values of ρ were from tenths of (Ω cm) to hundreds (Ω cm) at approximately the same density ($r \sim 1.5$ g/cm^3).

In other words, there is reason to suppose that in the resulting material, the electrical contacts between the grains are sufficiently reliable, and the porosity, in the first approximation, only slightly affects the charge transport mechanisms.

Note also that even in the early works on carbon sp^2 structures [20], it was noted that, for example, in pyrolytic carbons with the densities from $r = 1.20$ up to 2.26 g/cm^3, that is, from very porous highly disordered (almost amorphous) structures to dense highly oriented pyrolytic graphites, the temperature dependences of the resistivity is generally insensitive to such macroscopic factors as porosity or preferred orientation of microcrystallites and determined by the level of the crystalline perfection of the material (the size of microcrystallites and the degree of their ordering).

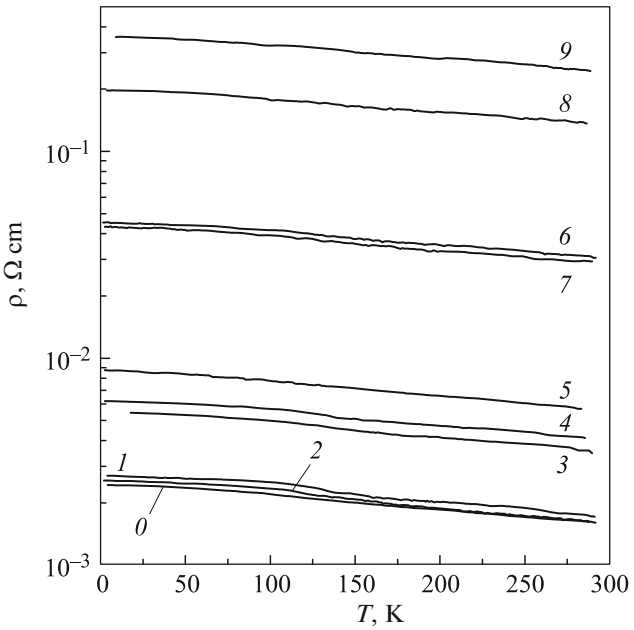

Fig. 7. Resistivity versus temperature of annealed samples with different ratios of components: (*0*) a sample without C_{60}, that is, pure pressed EG and (*1–9*) the samples with different initial weight ratios of C_{60} : EG: (*1*) 1 : 16, (*2*) 1 : 8, (*3*) 1 : 4, (*4*) 1 : 2, (*5*) 1 : 1, (*6*) 2 : 1, (*7*) 4 : 1, (*8*) 8 : 1, and (*9*) 16 : 1.

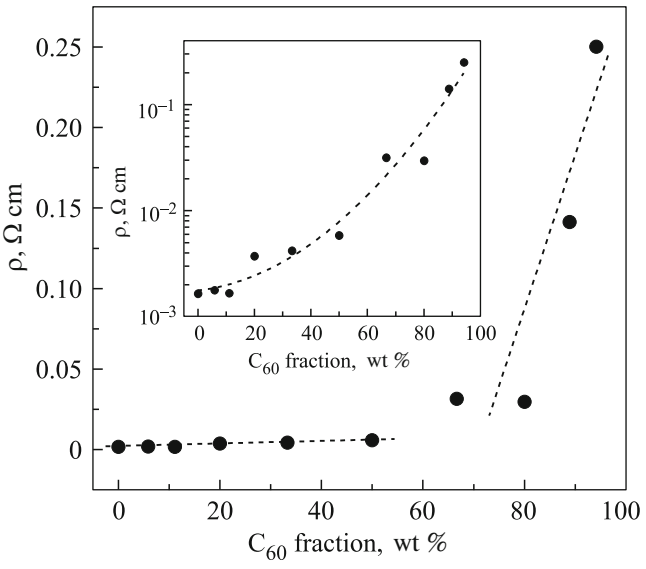

Fig. 8. Resistivity of the samples at $T = 273$ K, depending on the relative proportion of C_{60}. Inset is the dependence in a semilogarithmic scale. Dashed lines are drawn for orientation.

In view of the circumstances mentioned above, to account of porosity, we used simple multiplication of the electrical resistivity obtained in the experiment for real porous sample ρ_{exp} to the corresponding numerical coefficient, that is,

$$\rho_0 = \rho_{exp}(1 - P), \quad (5)$$

where ρ_0 was the resistivity of nonporous sample of the same material.

3.3. Electrical resistivity. The temperature dependences of $\rho(T)$ of the samples with different concentrations of C_{60}, taking into account the porosity calculated from Eq. (5), are presented in Fig. 7. It can be seen that the value of ρ increases with an increase in the proportion of fullerenes. Figure 8 demonstrates the dependence in a linear scale; it is also presented in a semilogarithmic scale in the inset for illustrative purposes. The dashed lines in Fig. 8 and the insert are given for orientation. Figures 7 and 8 represent the data obtained on all samples, except for pure C_{60}, due to its high resistance caused by the following circumstances.

Molecular crystals C_{60}, which are characterized with a band gap of $E_g = 1.5–2.3$ eV (according to different authors [21]), are known as *n*-type semiconductors; however, in practice they are insulators with $\rho \sim 10^6–10^7$ Ω cm. With increasing degree of disorder, ρ also increases. In all cases in air (that is, under exposure to oxygen), ρ increases by three to six orders of magnitude or more, reaching values $\sim 10^{14}$ Ω cm. In polymers obtained by compression of C_{60} powders, the magnitude of ρ decreases. For example, after such a procedure, it decreased by four orders of magnitude when the pressure reached 20 GPa, and it remained virtually unchanged until pressure of 8 GPa [22]. Therefore, the temperature dependence of ρ in various bulk C_{60} samples is often measured at $T > T_{room}$. For lower temperatures, films are typically used. For our pressed samples of C_{60}, the experimental estimates give the values of $\rho > 10^{12}$ Ω cm. Materials such as C_{60} + EG with a higher concentration of C_{60} than in the samples studied in the present work are considered rather high-resistance.

Overall, the data in Figs. 7 and 8 are typical of the material consisting of two components, characterized by high and low electrical conductivity. In this composite, there is a set of elements, the electrical conductivity of which varies substantially. The most conductive phase is probably a network formed by compacted and interconnected EG particles, that is, a medium such as EG + EG, and the most high-resistance (dielectric) phase is likely formed by fullerene molecules bound to each other by van der Waals forces, that is, a medium of $C_{60}–C_{60}$. As there is a covalent bond between C_{60} molecules and the environment, the material contains appreciable amounts of conductive phases such C_{60} + C_{60} (fullerene polymers) and C_{60} + EG (C_{60} molecules or units bound to the carbon matrix to form conductive circuits such as C_{60} + EG + C_{60} + EG). In any case, the most conducting phase

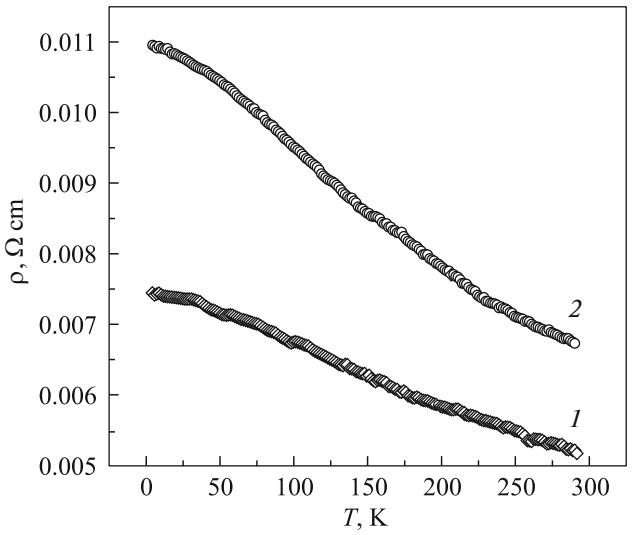

Fig. 9. Dependence of ρ(*T*) for two samples identical in composition of C_{60} : EG = 1 : 1: (*1*) nonannealed sample and (*2*) annealed sample.

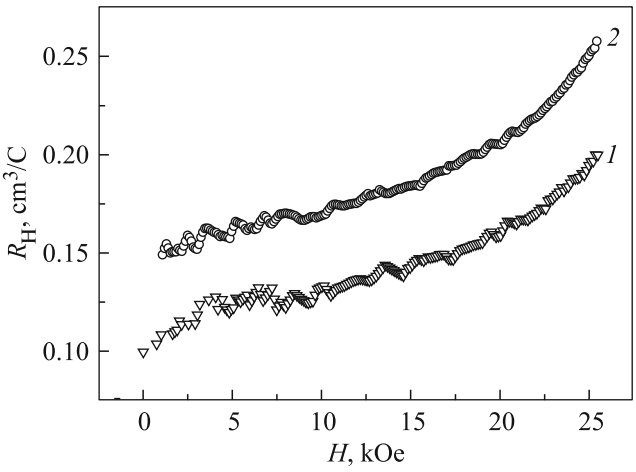

Fig. 10. Dependence of the Hall constant on the magnetic field strength for the same samples as in Fig. 9; $T = 77$ K.

present in the material in sufficient quantities will shunt all others. Because the material is generally quite low-resistance, the curves in Figs. 7 and 8 reflect the nature of the conductive component. A decrease in its concentration results in an increase in the resistance of the composite (Fig. 8).

3.4. Effect of annealing. The samples of type C_{60} + EG were strong enough at for all ratios of the components. They can easily withstand annealing at temperatures up to 650°C for several hours, without losing strength, completely without changing their shape, mass, and volume, and also maintaining the initial matte sheen of the surface (even point damages of the surface were not found). It can be assumed that the porosity remains practically unchanged upon annealing. At the same, the resistivity increased by approximately 30–60% in all the annealed samples (depending on the measurement temperature), as illustrated in Fig. 9, where the typical dependences of ρ(*T*), calculated from Eq. (5), are given. The Hall constant at $T = 77$ K in the synthesized samples is positive and depends on the value of *H* (though rather weakly), which indicates the presence of two subsystems of charge carriers, mainly holes. Their concentration n_h was evaluated by equation

$$R_H = 1/en_h,$$

(where *e* is the electron charge), that gives at $H = 0$, for example, for the composition of C_{60} : EG = 1 : 1 (Fig. 10), the values of $n_h = 6.3 \times 10^{19}$ cm^{-3} in the nonannealed sample and $n_h = 4.2 \times 10^{19}$ cm^{-3} in the annealed sample. Using the expression for conductivity

$$\sigma = 1/\rho = en_h\mu_h,$$

we obtain the corresponding evaluations of mobility, that is, $\mu_h = 14$ and 15 cm^2 (V s)$^{-1}$. In other words, the electrical resistance increases in the annealing of samples mainly due to a decrease in the concentration of mobile charge carriers. The reason for this may be a break of certain amount chemical bonds in the structure among the most stressed, which can lead to the appearance of additional traps of charge carriers.

Note also that according to Figs. 7 and 9, the temperature coefficient of resistance of the material is negative; that is, the value of ρ increases monotonically with decreasing temperature of the samples, and rather weakly (on average by approximately 1.5 times over the entire temperature range). This behavior, along with the *p* type of conductivity at a fairly high concentration of charge carriers and their low mobility, is characteristic of disordered graphite systems such as, for example, nanoporous [23] or biomorphic [24] modifications of carbon.

4. CONCLUSIONS

A composite carbon material is prepared and tested, in which fullerenes are placed for the first time into a matrix of exfoliated graphite. The samples were prepared by thermal treatment at 550–650°C of initial mechanical mixtures of C_{60} polycrystalline powders with EG particles at different weight ratios of C_{60} and EG, their pressing at a pressure of 0.7 GPa, and annealing the shaped monolithic samples at the same temperatures.

The porosity of the samples is assessed; the temperature dependence of their resistivity, the field dependences of the Hall constant, the spectra of the optical transmission in the range of frequencies of the vibrational modes of C_{60} molecule are measured and analyzed; and the effect of annealing is evaluated.

It is shown that IR spectra are significantly different from the original spectra of free C_{60} molecules, and the electrical resistivity increases slowly with decreasing temperature and greatly depends on the ratio of components. The value of ρ is in the range of units of mΩ cm to tenths of Ω cm. The concentration of charge carriers (mainly holes) is ~10^{19} to 10^{20} cm^{-3}.

Based on these results, it was concluded that covalent bonds are formed in the synthesized material between fullerenes and the environment; the material at the used ratios of the components can be attributed to metal systems with structural disorder.

ACKNOWLEDGMENTS

The work is partially supported by the Russian Foundation for Basic Research, project no. 14-03-00496, and the Program of the Presidium of the Russian Academy of Sciences, project no. P-20.

REFERENCES

1. V. I. Berezkin, *Carbon: Closed Nanoparticles, Macrostructures, and Materials* (ARTEGO, St. Petersburg, 2013) [in Russian].
2. Q. Z. Xue and X. Zhang, Carbon **43**, 760 (2005).
3. I. Lazar and G. Lazar, J. Non-Cryst. Solids **352**, 2096 (2006).
4. O. Gunnarson, Rev. Mod. Phys. **69**, 575 (1997).
5. V. Buntar and H. W. Weber, Supercond. Sci. Technol. **9**, 599 (1996).
6. V. I. Berezkin, JETP Lett. **83** (9), 388 (2006).
7. V. I. Berezkin and V. V. Popov, Phys. Solid State **49** (9), 1803 (2007).
8. A. S. Fialkov, *Carbon: Interlayer Compounds and Carbon-Based Composites* (Aspekt, Moscow, 1997) [in Russian].
9. *A Handbook of Chemist*, Ed. by B. P. Nikol'skii (GNTIKhL, Leningrad, 1962), Vol. 1 [in Russian].
10. B. Sundqvist, Adv. Phys. **48**, 1 (1999).
11. *Quasicrystals, Networks, and Molecules of Fivefold Symmetry*, Ed. by I. Hargittai (VCH, New York, 1990).
12. D. D. Klug, J. A. Howard, and D. A. Wilkinson, Chem. Phys. Lett. **188**, 168 (1992).
13. M. Matus and H. Kuzmany, Appl. Phys. A **56**, 241 (1993).
14. M. C. Martin, X. Du, J. Kwon, and L. Mihaly, Phys. Rev. B: Condens. Matter **50**, 173 (1994).
15. M. S. Dresselhaus, G. Dresselhaus, and P. C. Eklund, *Science of Fullerenes and Carbon Nanotubes* (Academic, San Diego, California, 1996).
16. M. E. Kozlov and K. Yakushi, J. Phys.: Condens. Matter **7**, L209 (1995).
17. V. A. Davydov, L. S. Kashevarova, A. V. Rakhmanina, V. M. Senyavin, R. Ceolin, H. Szwarc, H. Allouchi, and V. Agafonov, Phys. Rev. B: Condens. Matter **61**, 11936 (2000).
18. A. V. Eletskii and B. M. Smirnov, Phys.—Usp. **38** (9), 935 (1995).
19. M. P. Shaskol'skaya, *Crystallography* (Vysshaya Shkola, Moscow, 1984) [in Russian].
20. C. A. Klein, Rev. Mod. Phys. **34**, 56 (1962).
21. T. L. Makarova, Semiconductors **35** (3), 243 (2001).
22. Y. Saito, H. Shinohara, M. Kato, H. Nagashima, M. Ohkohchi, and Y. Ando, Chem. Phys. Lett. **189**, 236 (1992).
23. V. V. Popov, S. K. Gordeev, A. V. Grechinskaya, and A. M. Danishevskii, Phys. Solid State **44** (4), 789 (2002).
24. V. V. Popov, T. S. Orlova, and J. Ramirez-Rico, Phys. Solid State **51** (11), 2247 (2009).

Translated by O. Zhukova